# Oscillations of a Monsoon System. Part I. Observational Aspects

T. N. KRISHNAMURTI AND H. N. BHALME

*Department of Meteorology, Florida State University, Tallahassee 32306*

(Manuscript received 26 April 1976, in revised from 17 June 1976)

ABSTRACT

In this paper the elements of a monsoon system are defined, and its oscillations are determined from spectral analysis of long observational records. The elements of the monsoon system include pressure of the monsoon trough, pressure of the Mascarene high, cross-equatorial low-level jet, Tibetan high, tropical easterly jet, monsoon cloud cover, monsoon rainfall, dry static stability of the lower troposphere, and moist static stability of the lower troposphere. The summer monsoon months over India during normal monsoon rainfall years are considered as guidelines in the selection of data for the period of this study. The salient result of this study is that there seems to exist a quasi-biweekly oscillation in almost all of the elements of the monsoon system. For some of these elements, such as the surface pressure field, monsoon rainfall, low-level cross-equatorial jet and monsoon cloudiness, the amplitude of this oscillation in quasi-biweekly range is very pronounced. For the spectral representation of the time series, the product of the spectral density times frequency is used as the ordinate and the log of the frequency as the abscissa. Dominant modes are also found in the shorter time scales (<6 days). A sequential ordering of elements of the monsoon systems for the quasi-biweekly oscillation is carried out in terms of their respective phase angle. The principal result here is that soon after the maximum dry and moist static instabilities are realized in the stabilizing phase, there occur in sequence an intensification of the monsoon trough, satellite brightness, Mascarene high, Tibetan high and the tropical easterly jet. Soon after that the rainfall maximum over central India, arising primarily from monsoon depressions, is found to be a maximum.

In the second part of this paper we offer some plausible mechanisms for these quasi-biweekly oscillations.

## 1. Introduction

In this paper we shall first define a number of elements of a broad-scale monsoon system (Fig. 1). We shall next examine important fluctuations in these elements during a year of normal monsoon rainfall. The purpose of this observational study is to document, with a limited sample of roughly 100 days of data, some characteristics of this active monsoon system. Because of the large variability in monsoon rainfall from one year to the next, this study is limited in its scope. During a year of normal rainfall, the long-term daily mean rainfall (averaged over calendar days for many years) fits the observed daily rainfall patterns closely. However, even in these years of near-normal monsoon rainfall, there are considerable variations in the intensity of the monsoon. In part, this variability must arise due to the passage of active monsoon disturbances such as "monsoon lows" and "monsoon depressions" and other transients. Part of this variability could be due to the interaction of the monsoon system with other circulations, i.e., inter-hemispheric interactions and interactions with systems in the Pacific. We furthermore feel that there probably also exists a natural oscillation of the broad-scale monsoon system, due to its own inherent dynamics.

After the onset of monsoon rainfall over India, which usually occurs in early June, one frequently notes periods of minor and large "breaks" in the monsoon rainfall. The break phenomenon is not well understood. Ramamurthy (1969) has published an exhaustive survey of the breaks in the monsoons covering an 80-year period, 1888–1967. During breaks the broad-scale surface pressure trough moves northward over much of the Indian subcontinent, westerly winds prevail and rainfall amounts over central India are small. Ramamurthy has used these characteristics in his definition of the breaks in the monsoon. He examined the months of July and August for the 80 years of weather records. The breaks last for roughly 3–5 days in July and August. In the 80 years of records, there were no breaks during 12 of these years; one break per year during 25 of these years; two breaks per year during 22 of these years; three breaks per year during 9 of these years, and 4 breaks per year during 2 of the 80 years. Thus, one or two major breaks in the monsoons is a frequent occurrence. Although the breaks in the monsoons define periods of major cessation of rainfall over central India, the rainfall records show many other short- and long-term fluctuations within active periods as well. This study is not aimed at studying the phenomenon of the breaks, exclusively; however, we feel that this study on the fluctuations of the monsoon system may provide some insights into the mechanisms of the

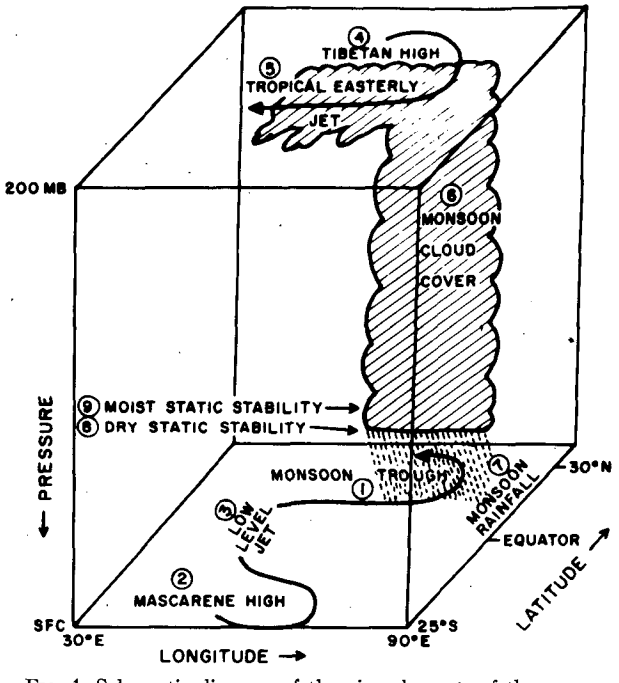


FIG. 1. Schematic diagram of the nine elements of the monsoon system considered in this study.

breaks. Two other relevant studies in this area are those of Murakami and Frydrych (1974) and M. Murakami (1976), both involving the monsoon. Theoretical aspects of the oscillation have been studied by Murakami and Frydrych (1974). Detailed observational studies of monsoons were recently presented by M. Murakami (1976). In this observational study Murakami noted both 5-day and 15-day oscillations in the pressure and motion fields. The latter was also identified as a period that distinguishes active from the inactive periods of the monsoons. These findings are quite consistent with our findings portrayed in the phase diagram. Murakami's study relates to the year 1962, another year with near-normal rainfall.

In this first part of a two-part paper, we present observational evidence of certain interesting oscillations of the monsoon system. In the second part we shall present radiative, dynamical and interactive aspects of the monsoons and thus offer an explanation for these monsoon fluctuations.

## 2. The broad-scale monsoon system

The broad-scale monsoon system is here defined by the following nine parameters (see Fig. 1).

### 1) MONSOON TROUGH

This is the low-pressure trough at sea level that is a part of the global equatorial trough of the northern summer season. Over land areas the equatorial trough extends from West Africa to the east coast of Indochina in this diagram. Fig. 2 illustrates the monsoon trough over northern India and is a July mean sea level isobar field.

### 2) MASCARENE HIGH

This is a high pressure area south of the equator and is also illustrated in Fig. 2. Its name comes from the Mascarene Islands east of Madagascar. The center

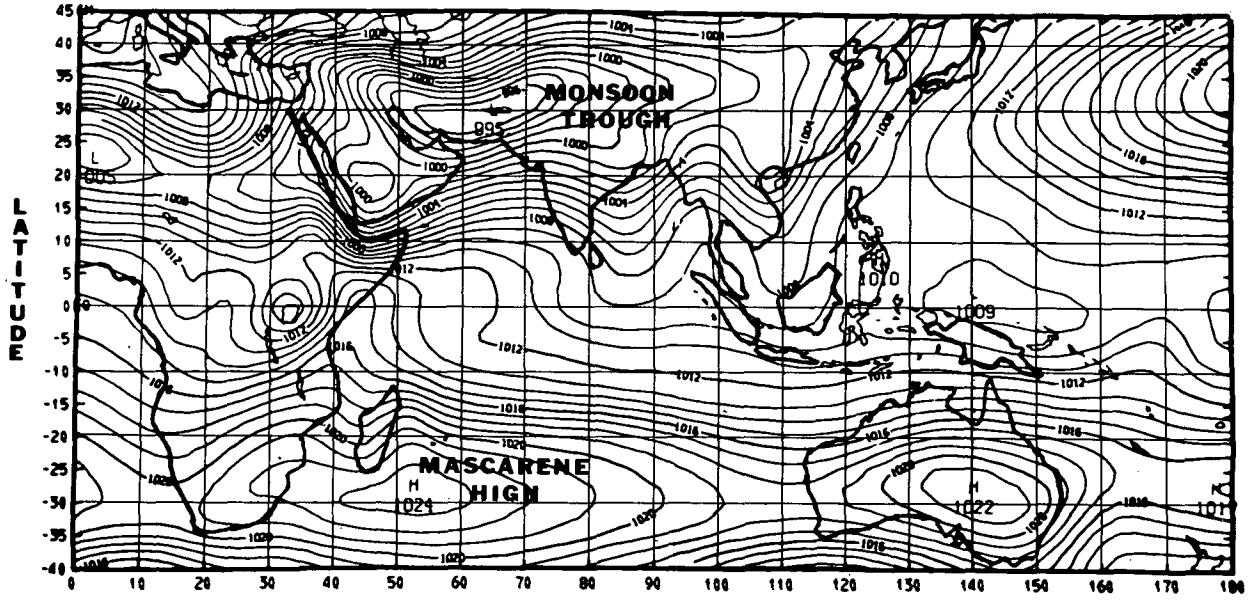


FIG. 2. Mean sea-level pressure for July (courtesy of Henry Van de Boogard).

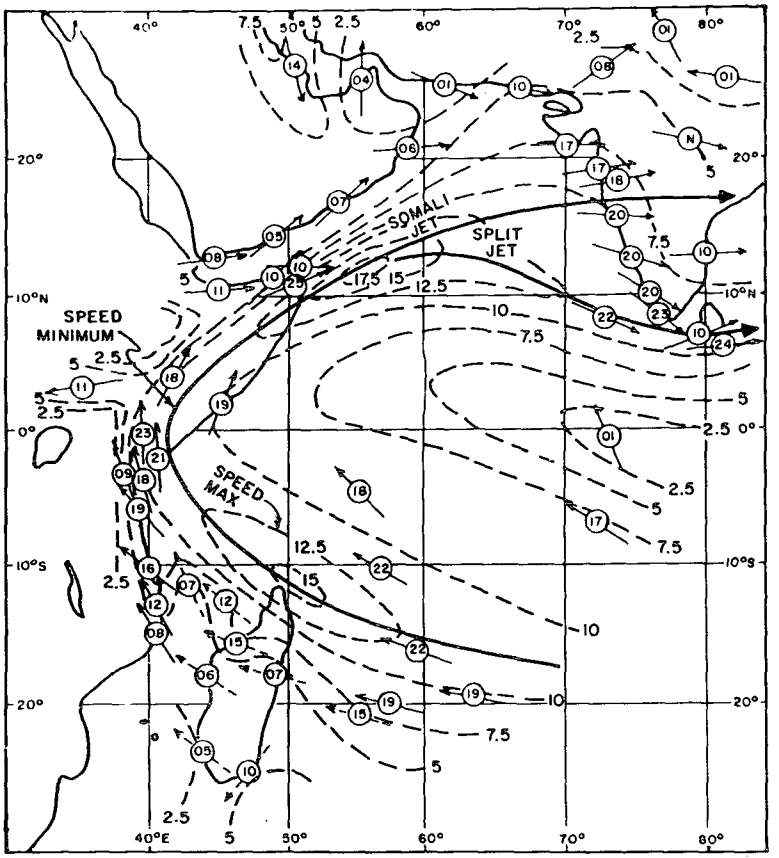


FIG. 3. Wind field at 1 km for August over the Arabian Sea–Indian Ocean region based on Findlater (1971). Isopleths are in meters per second. Station values within circles are in knots. The solid line indicates the axis of the low-level jet.

of this anticyclone is located near 30°S, 50°E. Synoptic meteorologists and operational weather forecasters in these regions have long recognized that this high pressure area has some importance during the monsoon months, although no definitive analysis of its importance has been illustrated.

### 3) LOW-LEVEL CROSS-EQUATORIAL JET

This is a well-known northern summer low-level jet. Its importance has been recognized since the observational studies of Findlater (1969a,b, 1971). Fig. 3 shows the 1 km wind field during August, based on Findlater's work. The jet has maximum winds near the 1.5 km level. It is known to occasionally have speeds of the order of 100 kt near Madagascar and off the Somali coast. It is a very narrow jet (both horizontally and vertically); its monthly mean vertical structure east of the Kenya highlands is shown in Fig. 4 (Findlater, 1971). The jet is confined close to the mountains and the western boundary effect of the east African highlands is recognized to be important for its dynamics. A simulation of this jet from a state of rest was recently presented by Krishnamurti *et al.* (1976). They showed that given a lateral forcing near 75°E, the flows over the domain of Fig. 3 can be somewhat realistically simulated if the beta effect and the bottom topography are included in a simple adiabatic primitive equation model.

The axis of the low-level jet begins to move northwestward in February (Fig. 5) and reaches the east African highlands by June. Thereafter its position remains steady for several months. This jet, furthermore, is known to become most intense during the months of June, July and August. During these months the axis of the jet downstream from the Somali coast is observed to split into two branches (Fig. 5). Krishnamurti *et al.* (1976) have analyzed the "split of the jet" problem from observations and from their simulations and concluded that this split over the Arabian Sea may be a consequence of barotropic instability of the Somali jet.

### 4) TIBETAN HIGH

This is a large anticyclone that is known to have its largest amplitude near 200 mb during the northern summer months. Its behavior has been illustrated by Flohn (1968), Krishnamurti and Rodgers (1970), Krishnamurti (1971), Krishnamurti *et al.* (1973), and

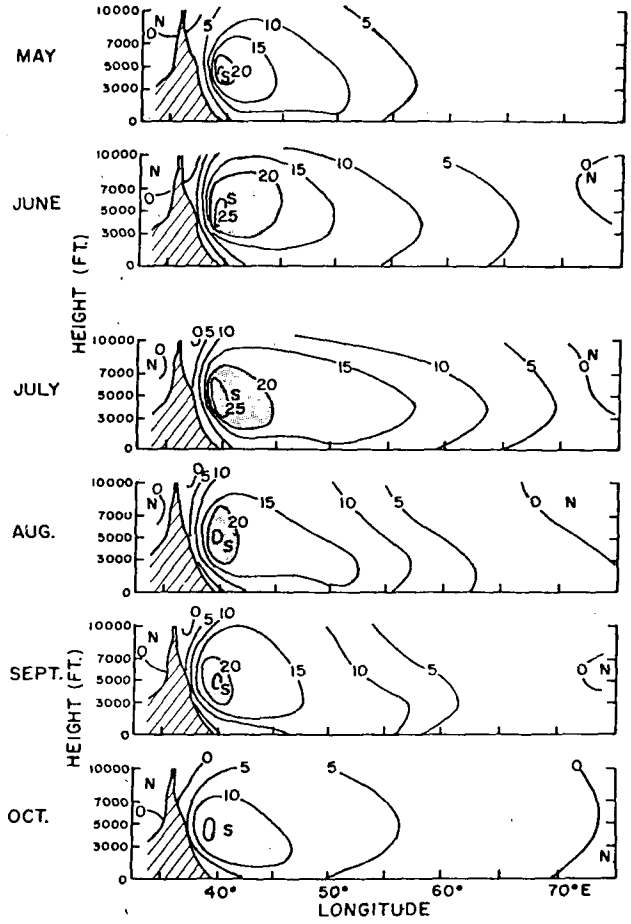


FIG. 4. Zonal vertical cross section of the monthly mean meridional wind speed near the equator, following Findlater (1971). Areas of wind speed>20 kt are shaded. The topography of the Kenya highlands is shown cross-hatched.

many others. Fig. 6 shows the monthly mean 200 mb flows over our region of interest. The upper anticyclone first forms in April just to the north of Borneo. In May it is located over southern Indochina, by June it is found over the northern part of Burma, and thereafter it moves over the Tibetan highlands. As shown in the monthly mean maps this anticyclone starts moving south-southeastward in September, and is found over Malaysia in November; thereafter it is known to lose its identity. In this paper we shall be concerned with short-period oscillations of the Tibetan high and the other parameters. The broad annual cycle illustrated here is of some interest, although it is not very well understood at present. It is furthermore of interest to note that the clockwise gyre defining the low-level jet moves northwestward over the Arabian Sea between April and July (Fig. 5) and the upper anticyclone over Indochina also moves northwestward toward Tibet during the same months (Fig. 6). The combination of the Tibetan high and the monsoon trough at sea level is accompanied by warm hydrostatic tropospheric columns over northern India and over the foothills of the mountains. The warm troposphere is another important feature of this total broad-scale monsoon system.

### 5) TROPICAL EASTERLY JET

One of the most fascinating features of the monsoon system is the upper tropospheric tropical easterly jet near 150 mb. This jet has winds of roughly 80–100 kt with the strongest winds being found just to the west of the southern tip of India over the Arabian Sea. Portions of this jet may be seen in Fig. 6. The jet forms in the monsoon month of June and is present until September. Fig. 6 illustrates a typical 200 mb map showing the wind field and the large horizontal extent of this wind system. The observational aspects of this jet have been investigated by Koteswaram (1961) and Krishnamurti (1971). It has also been modeled by Murakami *et al.* (1970).

In this zonally symmetric monsoon model the atmosphere starts from a state of rest. The model is two-dimensional in the meridional vertical plane. Nine vertical levels in the so-called "sigma frame" are used. The dependent variables of this system include horizontal and vertical velocity components, pressure, temperature and a moisture variable. Sea surface temperature is prescribed south of 10°N with land to the north where smoothed mountains are included; a detailed heat balance of the earth's surface is estimated during the course of the model simulation of

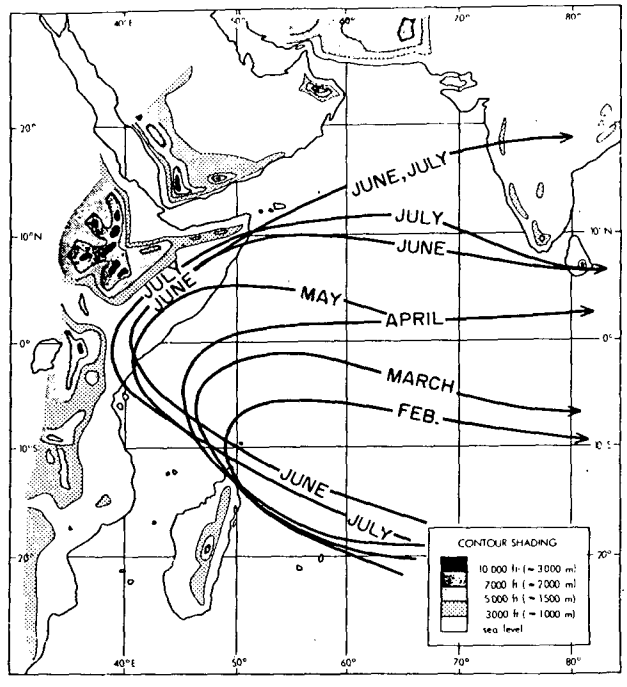


FIG. 5. Month-by-month progress of the axis of the low-level cross-equatorial jet. Note the split in the axis of the jet in June and July. The east African mountains are also indicated in this diagram.

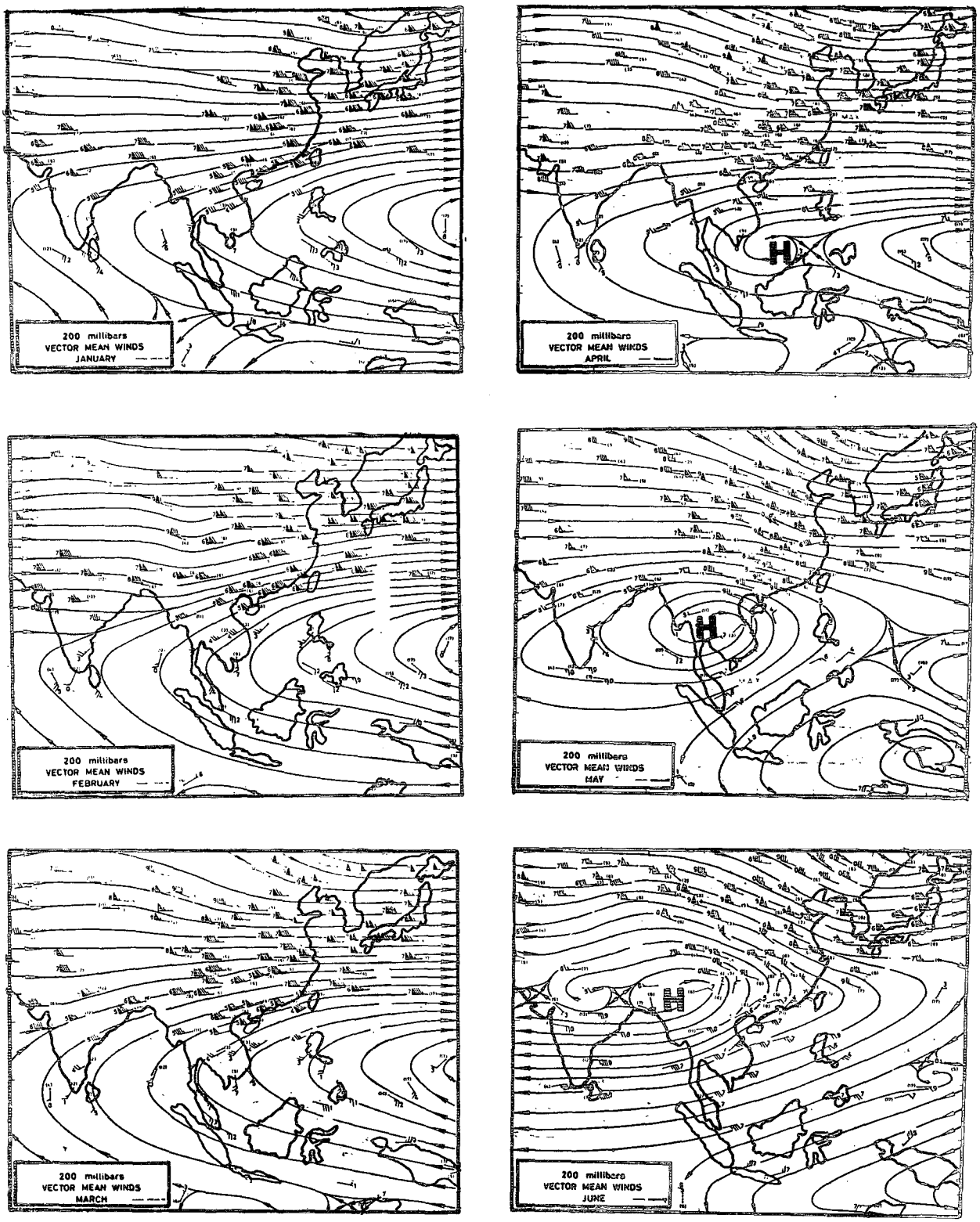


FIG. 6a. Monthly mean 200 mb wind field over Asia from January–June. Based on Chin and Lai (1974).

the monsoons. The heat balance estimates include calculation of the incoming and outgoing longwave radiation, incoming shortwave radiation, and fluxes of sensible and latent heat from land areas. This is found to be a crucial element in the numerical simulation of the zonally symmetric monsoons at 80°E.

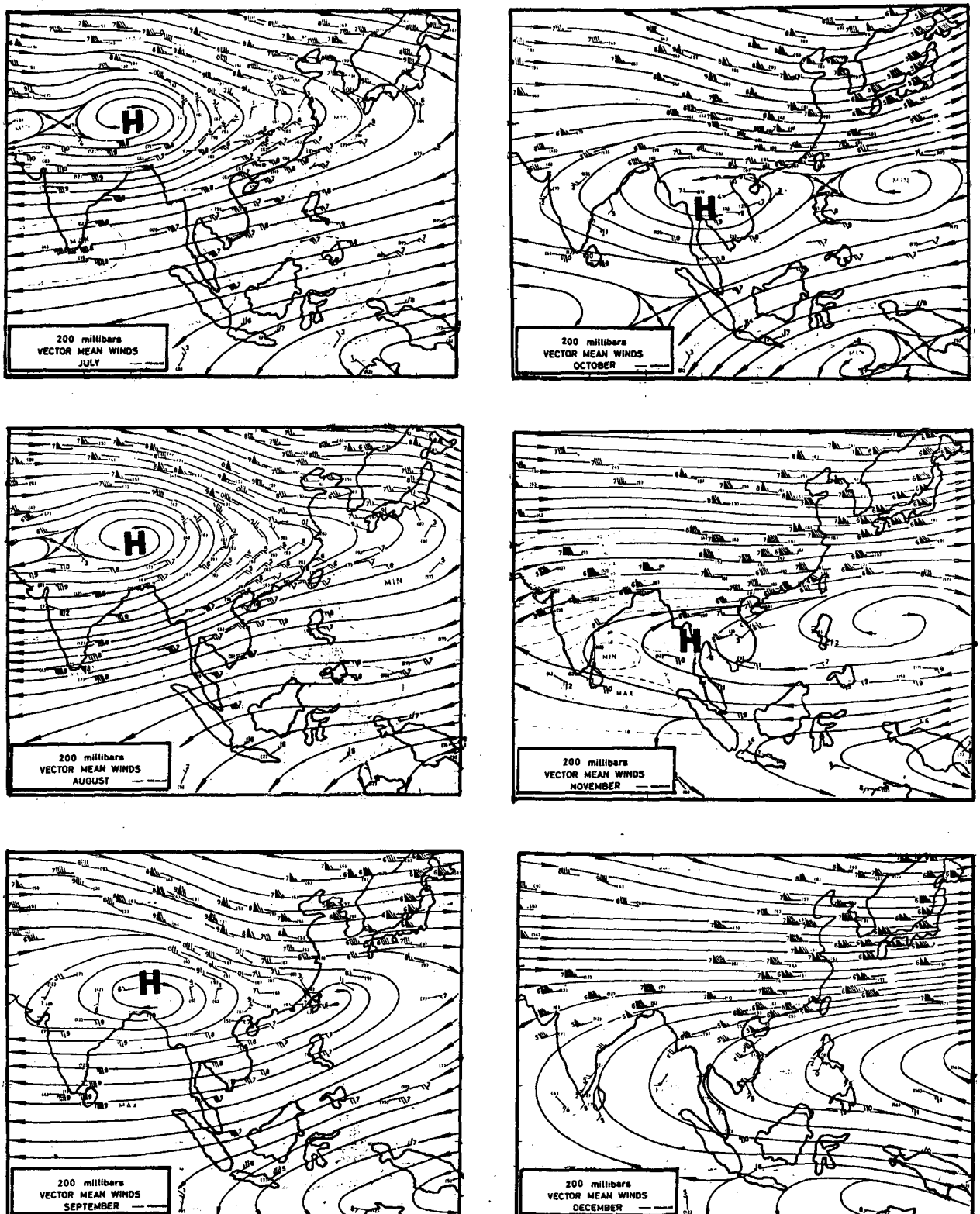


FIG. 6b. As in Fig. 6a except from July–December.

Dry and deep moist convection is included via the respective convective adjustment processes.

After some 80 days of integration this model reaches a statistical steady state. At this time kinetic energy in the model reaches a near steady state. This model is found to simulate many of the well known broad-scale features of the monsoons. Some of these are as follows:

- Southwest monsoon flows ($u>0$, $v>0$) in the lower troposphere below 600 mb north of the equator.
- Warm upper troposphere between 10° and 30°N.
- An anticyclone near 25°–30°N at 200 mb.
- A pronounced easterly jet (speeds 60–70 kt) near 14 km.
- A local Hadley cell with an ascending branch near 20°N and descending motions near the southern wall of the computational domain which was 2.5°S in this experiment. In another experiment, carried out at Florida State University, the southern wall was moved southward to 35°S and the descending motions shifted to near 25°S.

The energetics of this zonally symmetric monsoon are as follows:

- Heating generates available potential energy in the meridional plane, i.e., more net heating over land areas to the north and more net cooling to the south over the oceanic areas.
- Slow meridional Hadley-type vertical motions form with an energy exchange from the available potential energy to the kinetic energy of meridional circulations.
- Meridional kinetic energy is converted to kinetic energy of zonal motion (i.e., the tropical easterly jet). In the statistical steady state all of the energy received by zonal flows is lost by friction.

The model has a major limitation in that it is symmetric, thus the zonal flows cannot receive or lose energy to other horizontal scales. The model is akin to a giant sea breeze whose scale is so large that Coriolis turning for the meridional motions is substantial.

Another drawback of this broad-scale monsoon model is that no cloud feedback for the incoming shortwave radiation was included. In spite of the fact that condensation is included, the associated clouds do not influence the radiative heating calculations. We feel that the radiative effects of cloudiness may play a major role in the self-oscillation of the monsoon system. We shall discuss this further in Section 4 and this is the main theme of the second part of this paper.

In spite of the above-mentioned limitations, the Murakami *et al.* (1970) study was the first major contribution toward the understanding of the broad-scale monsoons. Because of its realistic simulation, we feel that part of the mechanism for the generation of the easterly jet must be contained in the physics of this model.

Kanamitsu *et al.* (1972) have examined the energetics of the easterly jet from global tropical data sets. Their view is somewhat different from that presented by Murakami *et al.* (1970) in that zonally asymmetric aspects of tropical circulations are considered. They found that zonally asymmetric as well as zonally symmetric parts of the net heating of the atmosphere are important in the tropical circulation. This goes with an east–west circulation (Krishnamurti, 1971), where they noted warmer air ascending over the monsoon land areas and relatively colder air descending over oceanic areas. The scale of this time-averaged east–west overturning was found to be related to the land-ocean configuration. As a consequence, kinetic energy is produced on a planetary scale (zonal wavenumbers 1 and 2) by these thermally direct vertical overturnings. The long waves have a very pronounced tilt and by removing westerly momentum from the latitudes of the easterly jet, they transfer kinetic energy to the zonal flows barotropically. A weak Hadley-type north–south overturning also produces zonal kinetic energy. The tropical easterly jet receives a large proportion of its energy in this manner. Thus, the asymmetric view of the easterly jet needs the planetary-scale quasi-stationary long waves as well as the local giant sea breeze of Murakami *et al.* (1970).

### 6) Monsoon cloudiness

The cloud cover over the monsoon region has been studied from surface records for well over 100 years. Records of such observations exist in the archives of the Indian Weather Service. Since 1960 satellite imagery has provided more detail over the oceanic regions around the Indian subcontinent. A global analysis of the satellite brightness for the entire tropical belt between 5° and 15°N was presented by Gruber (1974). Gruber utilized Hayashi's (1971) method of decomposing zonal waves into eastward and westward moving components. He found a 12.5-day mode which was predominantly a westward propagating wave with a scale of about 8000 km (wavenumber 5) for the northern summer. Our interest is in the satellite brightness and its fluctuation over the Indian subcontinent and adjoining areas. For this purpose, we present here two illustrations (Figs. 7a and 7b) contrasting a break monsoon day in July 1967 with one during active monsoons in the same month. We feel that the digital satellite brightness data provide a measure of the intensity of the monsoons.

### 7) Monsoon rainfall

In this paper we shall present monsoon rainfall over central India and its day-to-day variability

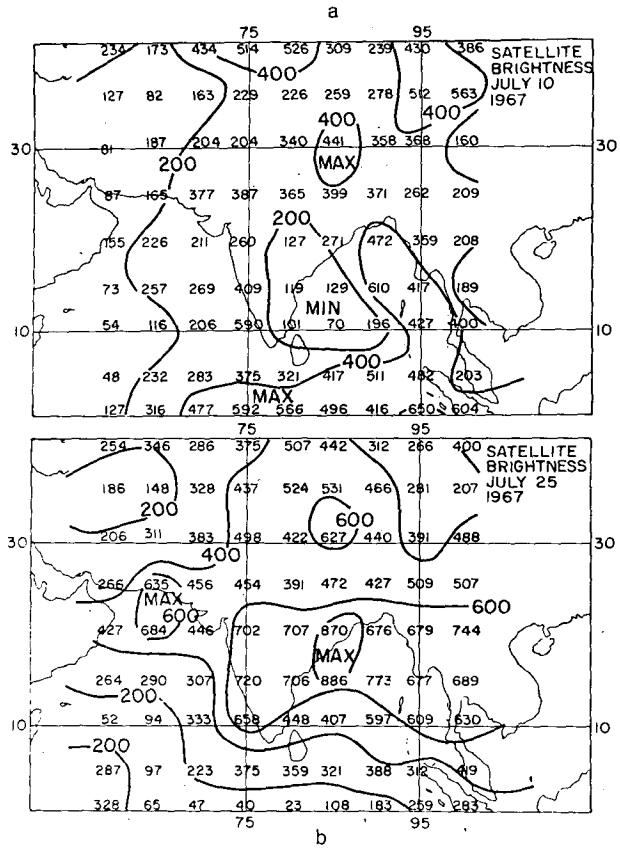


FIG. 7. Satellite brightness data over India on a "break" monsoon day (a) and an active monsoon day (b) during July 1967.

during an active monsoon year. As stated earlier, there are considerable variations in the monsoon rainfall from one year to the next. Fig. 8 contrasts the daily rainfall during 1972 and 1973 over central India (75°–85°E and 15°–25°N), i.e., during the drought year 1972 and the near-normal rainfall year 1973. The envelope in both of these diagrams is the daily normal based on 40 years of calendar-day averages. The drought year is characterized by much

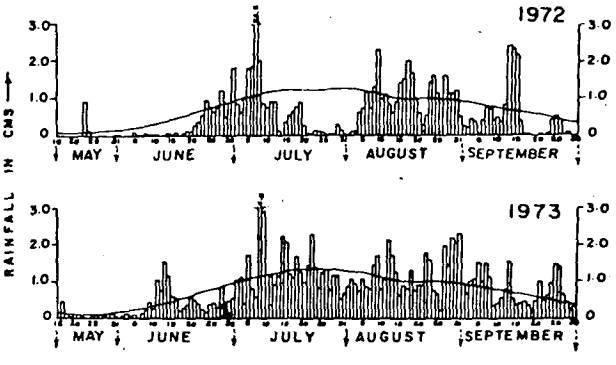


FIG. 8. Daily rainfall over central India (75°–85°E, 15°–25°N) during a drought year (1972) and a near-normal rainfall year (1973). The envelope line is the daily long-term normal rainfall.

longer breaks in the monsoon rainfall. During 1972 the break lasted for 13 days as compared to 3–5 days in most normal rainfall years.

#### 8) DRY STATIC STABILITY

In the monsoon belt over northern India during active and inactive rainfall periods, the surface heating goes from small to very high values due to solar insolation. The dry static stability fluctuates near the surface from stable to less stable or unstable values during these periods. This fluctuation may be related to the cloudiness cycle.

#### 9) MOIST STATIC STABILITY

Finally, we shall examine the fluctuation in a moist static stability parameter over the monsoon belt. A relevant parameter here is the change of moist static energy between the surface and 700 mb. This parameter should also exhibit stabilizing and destabilizing influences during active and inactive periods of the monsoon cycle. Warsh *et al.* (1971) have examined fluctuations in this parameter within the context of Atlantic disturbances.

## 3. Spectral analysis of the parameters of the monsoon system

### *a. Method*

In this section we present the results of a spectral analysis of daily records for the above-mentioned nine parameters of the monsoon system (Fig. 1). A homogeneous data set for the same period was not available for all of these elements. It was possible to obtain long records (3–4 months) during the summer monsoons for the years 1957, 1962 and 1967, which covered all of these elements. These years were characterized by active monsoons with near-normal rainfall amounts. The purpose of this analysis is to isolate any significant common factors that may be present in the oscillation of the total monsoon system (Fig. 1). To the best of the author's knowledge, such an integrated approach has not been pursued in previous studies. The first step in our analysis of the power spectral density consists of the removal of the root-mean-square linear trend from the raw data sets. In the monsoon months, a slow linear trend was noted in most of the raw data sets we present in this paper. Our numerical approach is the direct fast Fourier transform method essentially following Endlich *et al.* (1969). In the execution and analysis of the spectra, we have followed the earlier works of Wallace (1971), Yanai *et al.* (1968) and Zangvil (1975). The coefficients of the $\{x\}$ series are given by

$$X_k = \sum_{j=0}^{N-1} x_j e^{-i2\pi jk}, \quad k=0, 1, 2, \ldots, N-1, \qquad (1)$$

where $2N$ represents the number of data points and $N$ is the number of coefficients.

The power spectral estimate of the series is given by

$$G_{xk}=(2\Delta t/N)|X_k|^2,\ k=0, 1, 2, \ldots, N-1, \quad (2)$$

where $\Delta t$ is the time interval.

Smoothed estimates may be obtained by averaging $L$ contiguous raw estimates to yield

$$G_{xk}=L^{-1}\sum_{j=1}^{L} G_{x(k+j)}. \quad (3)$$

We also calculate the phase angle between two series. This involves an evaluation of the co-spectrum and the quadrature spectrum of two series from the cross-spectral density $G_{xyk}$. Given two series $\{x\}$ and $\{y\}$ their coefficients are first evaluated by the fast Fourier transform method, i.e., $X_k$ and $Y_k$, as in Eq. (1). The cross-spectral density for $\{x\}$ with respect to $\{y\}$ is given by

$$G_{xyk}=(2\Delta t/N)(X_k{}^*Y), \quad (4)$$

where the asterisk denotes a complex conjugate and $k$ takes on values $0, 1, 2, \ldots, N/2$. Here the subscript $k$ represents a frequency of $k/N\Delta t$. The co-spectrum $C_{xyk}$ and the quadrature spectrum $Q_{xyk}$ are, respectively, the real and the imaginary part of $G_{xyk}$, i.e.,

$$G_{xyk}=C_{xyk}-iQ_{xyk}. \quad (5)$$

The phase angle is given by

$$\theta_{xyk}=-(360°/2\pi)\tan^{-1}(Q_{xyk}/C_{xyk}). \quad (6)$$

Our primary interest in this paper is to illustrate the power spectral density of the elements of the monsoon system. The phase of only those elements will be illustrated for which data for the same year and period are available. We shall also follow the representation of Zangvil (1975) in our depiction of the power spectral density. Here the product of the power spectral density and the frequency is plotted along the ordinate and the log of the frequency along the abscissa. The advantage of this representation for meteorological power series has been discussed by Zangvil (1975).

### *b. Results of spectral analysis*

The raw data and their spectra for the nine elements of the monsoon system are presented for selected years where the monsoon rainfall was near normal.

#### 1) MONSOON TROUGH

Figs. 9a and 9b illustrate the sea level pressure and the monsoon trough spectrum, respectively. Table 1 shows the parameter region, period and years for which these calculations were carried out. The raw data indicate a gradual increase of the mean pressure, reflecting a seasonal change. For these months, IGY data of surface pressure were readily available. The rms linear trend was calculated to remove this seasonal change. The salient pressure oscillation in the monsoon trough is around 11.5 days. Another feature may be noted around 4.5 days. The oscillation near 12 days is very conspicuous in the raw data record of 92 days where it is easy to count 7–8 distinct peaks in the pressure of the monsoon trough

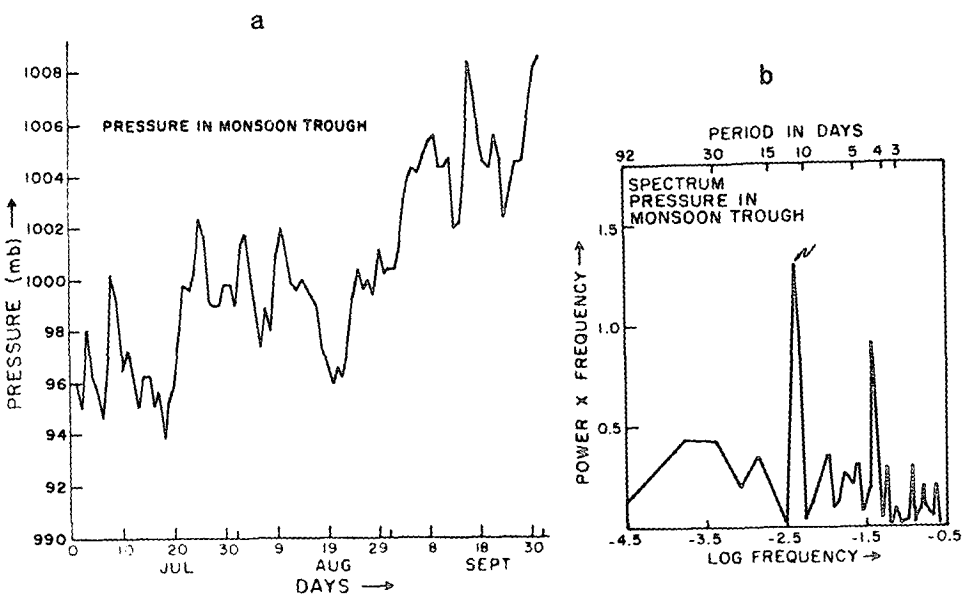


FIG. 9a. Daily mean sea level pressure over the monsoon trough. See Table 1 for the domain. The International Geophysical Year (IGY) data were used in this study. FIG. 9b. Power spectrum for the monsoon trough.

TABLE 1. Domains, data sources and periods for the various elements of the monsoon system.

| Parameter | Data sources | Data period | Number of days | Domain over which daily data is averaged |
|---|---|---|---|---|
| 1. Pressure in monsoon trough | IGY maps | July, August, September 1957, 1967 | 92 | 60° to 100°E<br>20° to 25°N |
| 2. Pressure in Mascarene high | IGY maps | July, August, September 1957, 1967 | 92 | 40° to 70°E<br>25° to 30°S |
| 3. Low-level jet | Findlater | July, August 1962 | 62 | Garissa, Kenya winds. Equator and 40°E |
| 4. Tibetan high | Krishnamurti and Rodgers (1970) | June, July, August 1967 | 92 | 50° to 130°E<br>17° to 35°N |
| 5. Tropical easterly jet | Krishnamurti and Rodgers (1970) | June, July, August 1967 | 92 | 2.5° to 10°N<br>55° to 75°E |
| 6. Monsoon cloud cover | Satellite brightness tapes (NCAR archives) | June, July, August 1967 | 92 | 0° to 25°N<br>60° to 100°E |
| 7. Monsoon rainfall over central India | India Meteor. Dept. | June, July, August 1967 | 92 | 73° to 82°E<br>12° to 25°N |
| 8. Dry static stability (1000–900 mb over north central India) | India Meteor. Dept. | June, July, August 1967 | 92 | Lucknow, Jodhpur, Nagpur |
| 9. Moist static stability (1000–700 mb over north central India) | India Meteor. Dept. | June, July, August 1967 | 92 | Lucknow, Jodhpur, Nagpur |

### 2) MASCARENE HIGH

The corresponding diagrams are presented in Figs. 10a and 10b. This data set covers the same IGY period as for the monsoon trough (Table 1). A pronounced linear trend is not conspicuously present in this data set which shows roughly 7–8 major oscillations in the pressure of this high. A broad and large power spectral density may be noted around 11.5 days and a major peak around 3.5 days.

### 3) LOW-LEVEL CROSS-EQUATORIAL JET

The data set and the spectrum are shown in Figs. 11a and 11b. One of the biggest problems here is the availability of data sets with long and complete records. In spite of our attempts to obtain detailed data sets for 3–4 months for east African weather stations in the vicinity of the low-level jet, we could not find continuous data sets. Much of the data contains large gaps. In this analysis we have used

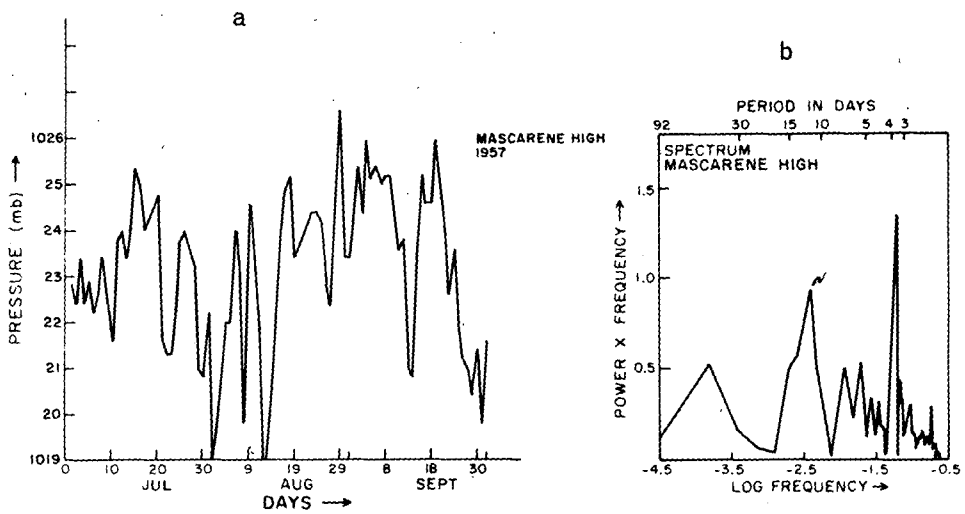


FIG. 10. As in Fig. 9 except over the Mascarene High.

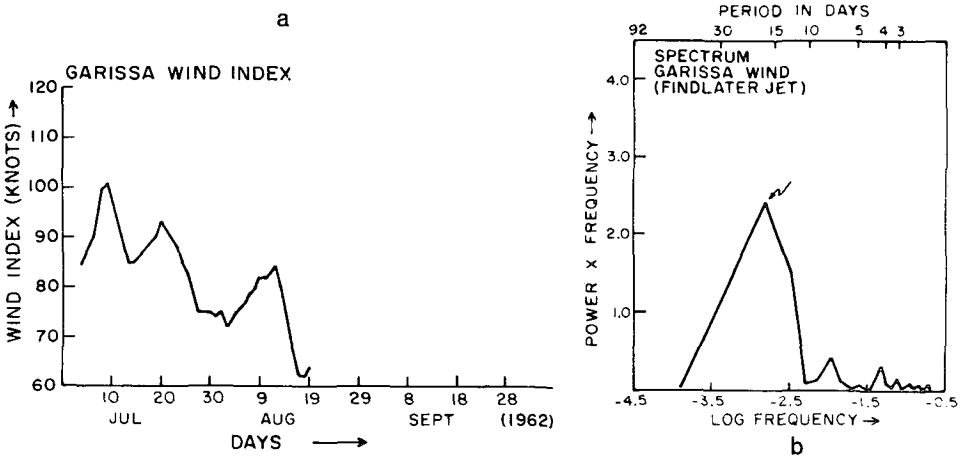


FIG. 11a. Data used for the power spectral analysis of the low-level cross-equatorial jet. See text for a definition of the wind index. See Table 1 for domain and period. FIG. 11b. Power spectrum for the cross-equatorial low-level jet.

the observations from Findlater's (1969a) work. This covers only a 62-day period (see Table 1) as compared to over 92 days of records for all other parameters. The following reservation is expressed on the Findlater wind index data. The wind index is a layer mean wind between 0.9 and 1.5 km. The vertically averaged vector mean wind is obtained from pilot balloon observations at Garissa, Kenya. Findlater's data, however, suffer from a time average which is somewhat undesirable. He had obtained 5-day overlapping running means to define his wind index. This procedure may have some influence on the spectra presented here, possibly by reducing the intensity of shorter period transients. Unfortunately, it was not possible to obtain raw data of these observations. The results of the spectral analysis of this data set (Fig. 11b) show a very pronounced peak around 15.3 days. This is also quite conspicuous in the data set illustrated in Fig. 11a. There is also some power in time scales between 3–6 days as well.

### 4) TIBETAN HIGH

The oscillation of the Tibetan high was first pointed out by Krishnamurti *et al.* (1973), but for the sake of completeness we present the results of that study here in Figs. 12a and 12b. The data set (Table 1) covers a period of 92 days during the summer of 1967. A seasonal buildup of the Tibetan high is reflected in the local mean value of the streamfunction illustrated in Fig. 12a. The spectral analysis (Fig. 12b) reveals a major peak near 3 days and another around 13.1 days.

### 5) TROPICAL EASTERLY JET

Data from the atlas of Krishnamurti and Rodgers (1970) were used in the spectral analysis of the total

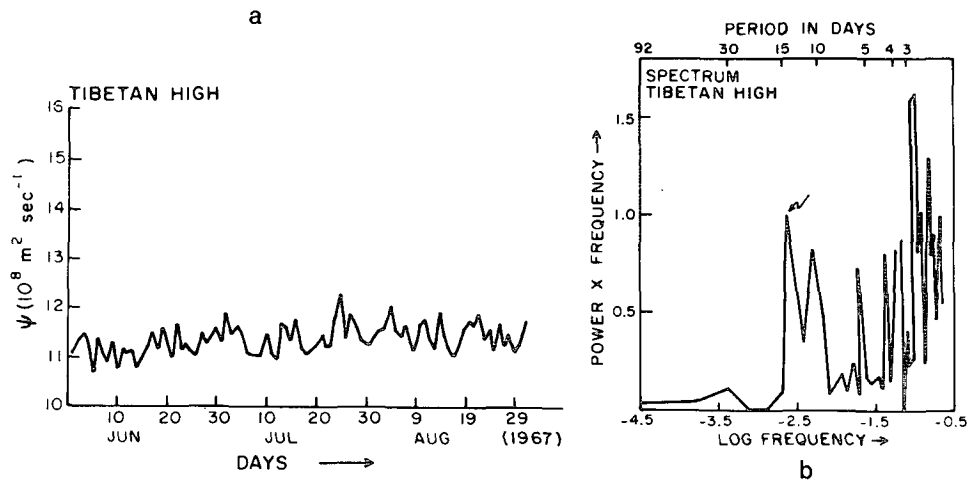


FIG. 12. As in Fig. 11 except for the Tibetan high. This data set is explained in Krishnamurti *et al.* (1973).

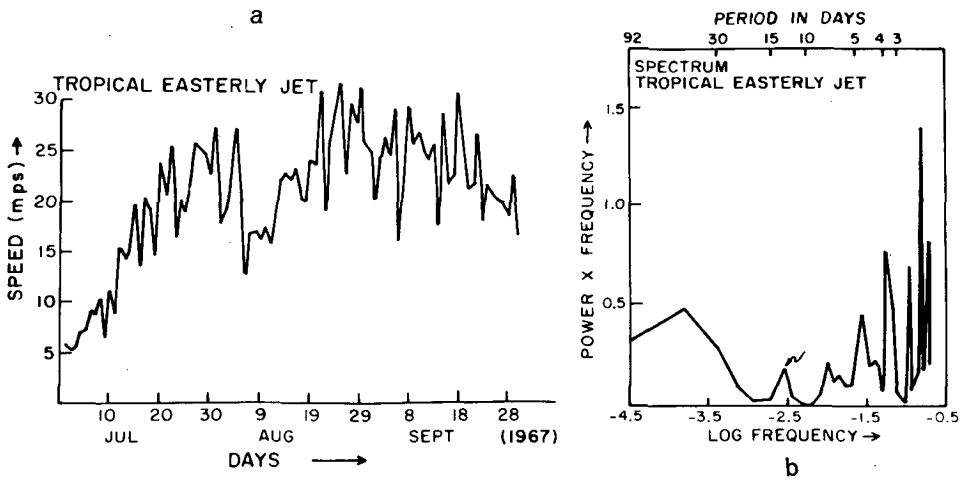


FIG. 13. As in Fig. 11 except for the tropical easterly jet. The data set is from Krishnamurti and Rodgers (1970).

wind at 200 mb for the region of the climatological wind maxima for 92 days during 1967 (see Table 1). The raw data illustrated in Fig. 13a show considerable day-to-day fluctuations in the intensity of this 200 mb jet. Although the spectral density illustrated in Fig. 13b shows a number of peaks with periods $<6$ days, we also note a distinct and isolated peak near 13.1 days. The large variability of the tropical easterly jet for periods $<6$ days may be a consequence of local barotropic instability of the jet. Kanamitsu *et al.* (1972) have examined the kinetic energy exchanges from zonal to other scales with this data set and found that there was a significant energy exchange from zonal to shorter waves. This result was also confirmed by Colton (1973) and by Zangvil (1975).

### 6) MONSOON CLOUD COVER

The satellite brightness data (see Table 1) for the same year and period during 1967 was utilized in this spectral analysis. The raw data are stratified between 1 and 1000 units. An overcast situation within an entire 5° latitude by 5° longitude is assigned 1000 units. The fractional coverage in these squares usually varies between 100 and 700 units during the monsoon months over northern India (Fig. 14a). The spectra of satellite brightness (Fig. 14b) reveals a number of peaks in the 1–4.5 day range, and a significant peak around 13.1 days.

### 7) MONSOON RAINFALL

The data set used for spectral analysis of the monsoon rainfall over central India is illustrated in Fig. 15a. These are daily rainfall totals for 1967 over a domain indicated in Table 1. A break in the monsoon occurred over India around 10 July (Ramamurthy, 1969). The rainfall during this year was near normal during most of the monsoon months. The spectrum of monsoon

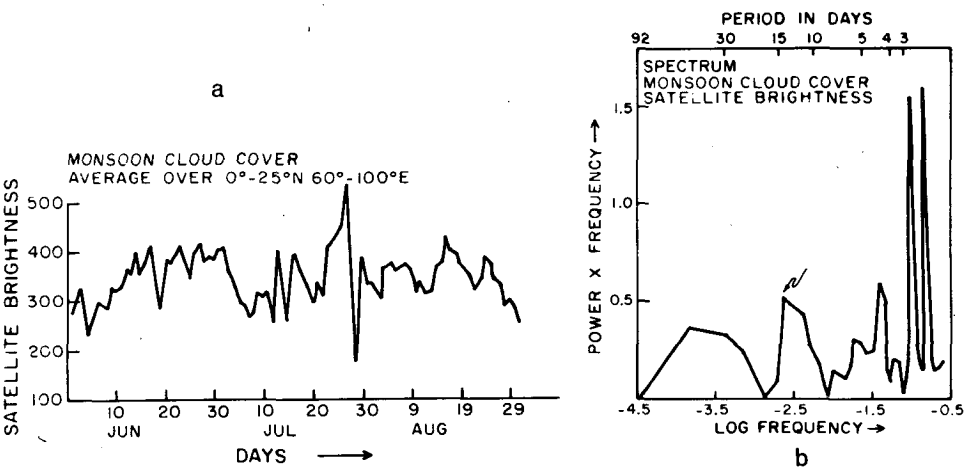


FIG. 14a. Satellite brightness data used in the spectral analysis. The domain over which the daily data was averaged is shown in Table 1. The text explains the units. FIG. 14b. Power spectrum for the satellite brightness.

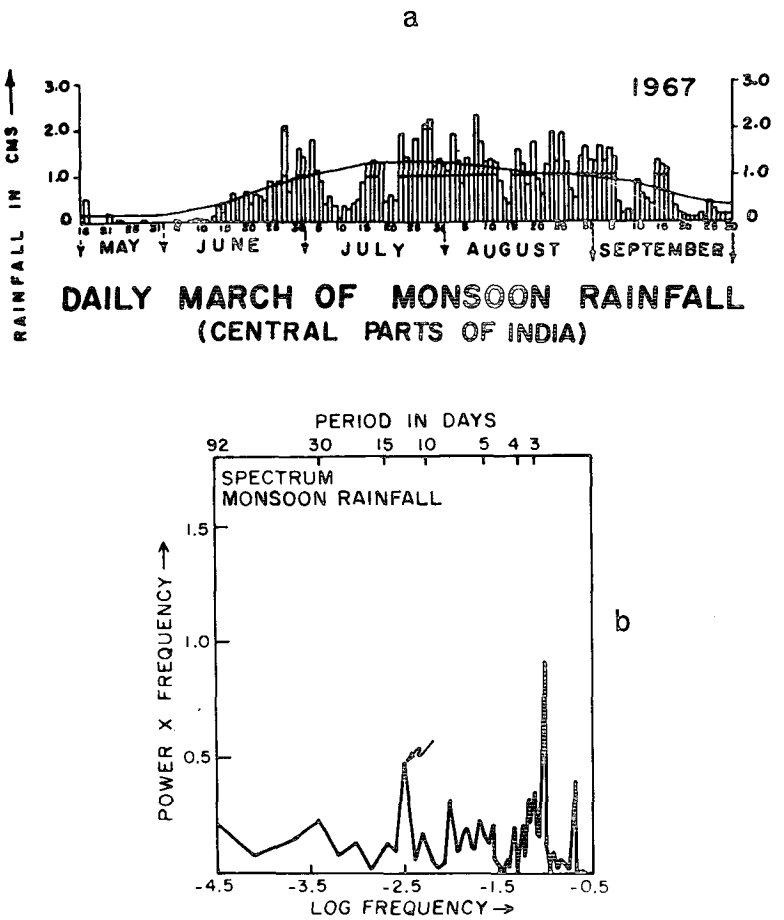


FIG. 15. Daily values of monsoon rainfall averaged over central India (a) and the power spectrum for monsoon rainfall (b).

rainfall shown in Fig. 15b shows two major peaks around 2 days and 13.1 days.

### 8) DRY STATIC STABILITY

The fluctuations in the dry static stability parameter are examined here, i.e.,

$$\Gamma_d = -c_p \frac{T}{\theta}\frac{\partial\theta}{\partial p} = -\frac{\partial}{\partial p}(gz+c_pT),$$

where $\theta$ is potential temperature, $T$ the temperature, $p$ the pressure and $gz+c_pT$ is the dry static energy. It is computed for three central Indian weather stations (Lucknow, Jodhpur and Nagpur) for the layer between 1000 and the 900 mb. A distance-dependent weighing about the centroid of the triangle formed by these stations was used to obtain the daily mean dry static energy (for 1700 local time) for each of the 92 days. The dry static stability parameter and its spectra are shown in Figs. 16a and 16b.

### 9) MOIST STATIC STABILITY

A moist static stability parameter is here defined by

$$\Gamma_m = -\frac{\partial}{\partial p}(gz+c_pT+Lq),$$

where $q$ is the specific humidity and $L$ the latent heat of condensation. The same three weather stations over north central India are considered here. The variability of the moist static stability and its spectrum are given in Figs. 17a and 17b. In the period range of less than 5 days considerable fluctuations in the dry and moist static stability were noted. Near the 5-day range, there is a pronounced peak in the moist static stability; we also note a significant peak around 15 days. These two peaks are not that pronounced for the dry static stability parameter. Similar peaks in the oscillations of the dry and moist static stability are found for period $<5$ days. These small-period oscillations are evidently due to disturbances (e.g., monsoon lows) which seem to stabilize and destabilize the atmosphere in the dry and the moist

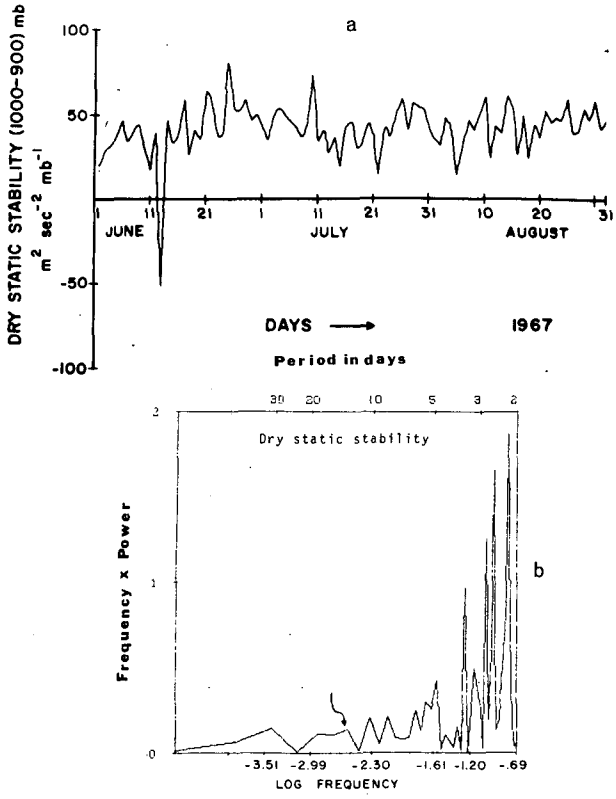


FIG. 16. Daily values of dry static stability averaged for three stations over central India for the vertical layer 1000–900 mb (a) and the power spectrum for the dry static stability (b).

sense at roughly the same frequency. In the 15-day period, the power for the dry static stability is quite small. The values of the dry static stability are positive and those of the moist static stability negative throughout the 92-day period, with two exceptions. On 13 July the dry static stability in the layer 1000–900 mb was negative for all three stations considered here. The moist static stability in the layer 1000–700 mb was positive on the 9th and 10th of June. After a careful inspection of the raw data we could not find any justifiable reasons for removing these features; hence, they were included in the time series. We feel that the layer 1000–900 mb is somewhat too deep to provide a realistic measure of dry static instability near the ground. The layer between 1000 and 700 mb is a representative depth for the moist static stability, since the minimum value of the moist static energy does occur near the 700 mb surface.

## 4. The relative phase of the quasi-biweekly mode

Here we shall examine the phase of the 13.1-day mode for 1967. In order to examine as many parameters as possible for the same year we used the operational weather maps of sea level isobars from the Indian and the Mauritius Weather Service for the first two items of Table 1. Thus, we were able to acquire a 92-day data set for all but the cross-equatorial low-level jet. The spectral analysis was performed for 8 of the 9 elements of Table 1 and the phase angle [Eq. (6)] was expressed relative to that of the dry static stability parameter. The phase diagrams are given in Figs. 18a and 18b, the former illustrating the relative phase during the stabilizing period of the 13.1-day mode and the latter the destabilizing portion of this cycle. For purposes of clarity, the two diagrams are shown separately, although one is merely 180° out of phase with the other.

Starting from a maximum dry static instability the following sequence of events in the 13.1-day cycle may be noted. The moist static instability reaches its maximum value before the other elements. The monsoon trough reaches its minimum low pressure value next, followed by a maximum in the satellite brightness indicative of broad-scale monsoon rainfall. The Mascarene high of the Southern Hemisphere reaches its maximum value roughly 1.5 days after the maximum intensity of the monsoon trough. The Tibetan anticyclone at 200 mb reaches its peak value in this cycle some 2 days after that. This is followed by an intensification of the tropical easterly jet at 200 mb and the maximum rainfall over central India is reached some 5.2 days after the maximum dry static instability is found over that region. It should

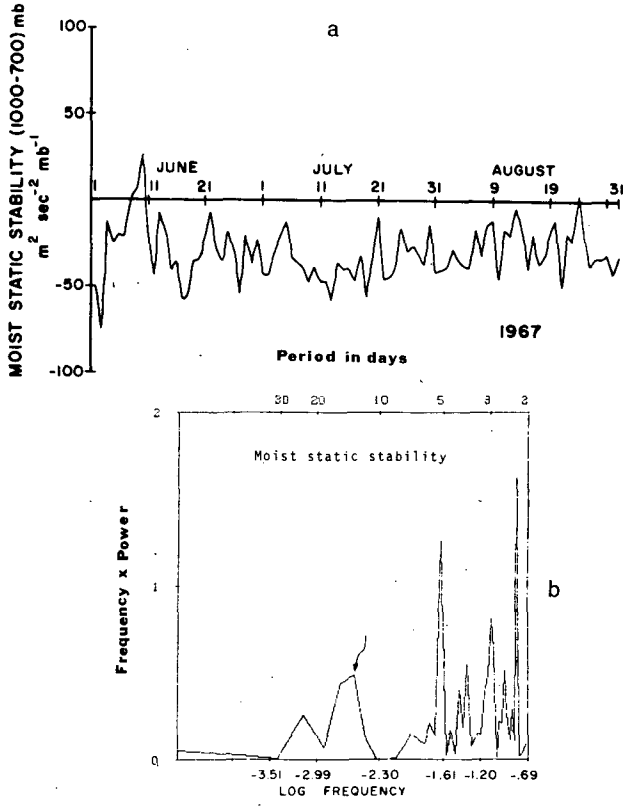


FIG. 17. As in Fig. 16 except for the moist static stability and the vertical layer 1000–700 mb.

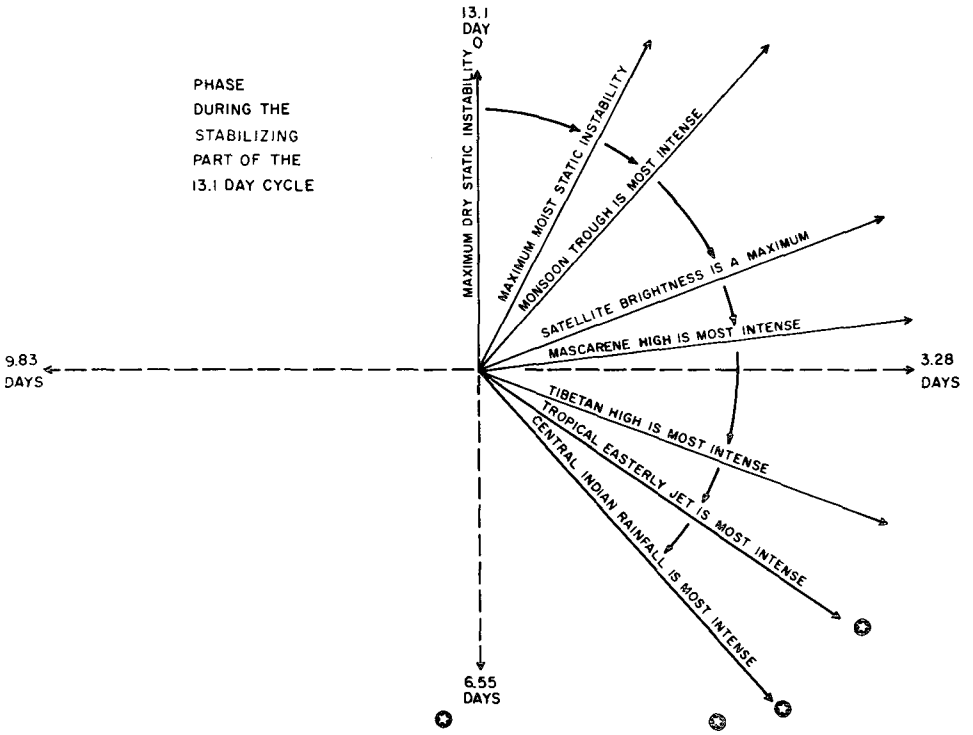


FIG. 18a. Phase diagram for the elements of the monsoon system during a stabilizing part of the 13.1-day cycle.

be noted that, although the power spectral density for the dry static stability parameter is small, the results were not changed by evaluating the cross spectra with respect to another reference parameter, such as the moist static instability. In the bi-weekly period the maximum intensity of the eight parameters presented in the phase diagram are mostly clustered during a 5-day period. Among these the phase of the

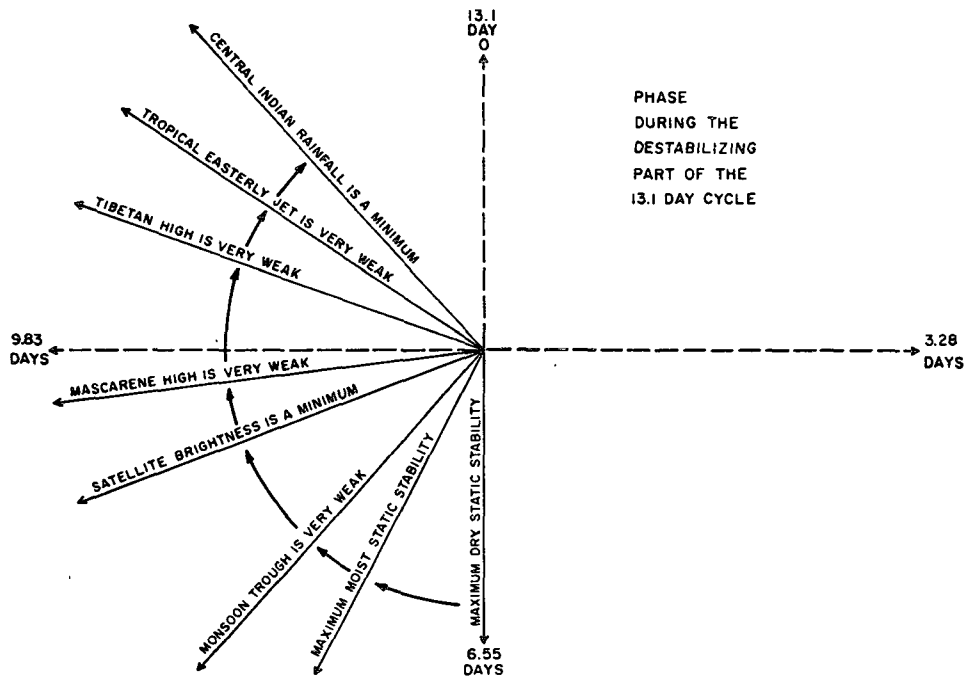


FIG. 18b. As in Fig. 18a except during a destabilizing part of the 13.1-day cycle.

dry and moist static instabilities lead the other parameters shown in Fig. 18.

The story of the sequential ordering of these various phenomena according to their phase is not an easy one to interpret. In these phase diagrams the reference line, i.e., day zero, is the time when the dry static instability reaches its maximum value for the 13.1-day mode. It is worth emphasizing here that the sequence of phase changes illustrated here refer only to the quasi-biweekly mode and not to other frequencies of the monsoon system. Short-term transients may not have a similar ordering of phase for these same elements of the monsoon system. Careful judgment should be exercised prior to any applications of the following tentative interpretations.

During periods of strong solar insolation and lack of large cloud cover, the dry static instability over central India increases. Most likely this period (around $t=0$) is characterized by shallow dry convection, large-scale subsidence over the middle and upper troposphere, and a gradual extension of the heat low toward central India.

The restoring of conditional instability over the tropics (Krishnamurti and Kanamitsu, 1973) is governed by factors such as large-scale subsidence, strong radiative and evaporative cooling near the top of the moist layer, and strong warming of the air near the ground. Large moist static instability is associated with a large minimum value of equivalent potential temperature near 700 mb that cannot be restored by horizontal advective processes alone. It is thus not surprising that large moist static instability is realized about a day after large dry instability.

The extension of the heat low toward central India is consistent with a subsequent deepening of the central pressure of the monsoon trough. As may be noted from Fig. 9a, there exists a linear trend of increasing central pressure of the monsoon trough as the monsoon season becomes very active. In fact, the central pressure is usually a minimum before the active monsoons, i.e., when a heat low prevails over large areas. Thus, we identify the oscillation of the monsoon trough between lower and higher values as an alternation between heat low conditions and moist monsoon conditions. Here the reference is to the large-scale monsoon troughs and not to smaller scale disturbances. When the dry static instability attains a maximum value, heat low conditions prevail and it is not surprising that a large-scale deepening of the surface pressure of the monsoon trough occurs soon thereafter. The next step in this cycle is a maximum value in the satellite brightness and widespread monsoon rainfall over a large area (Table 1). The widespread rainfall and associated latent heating would account for an intensification of a local meridional Hadley-type vertical overturning. The rising branch of this cell is over northeastern India and the sinking branch would be over a subtropical high which is the Mascarene high. The intensification of the Mascarene high may be a consequence of this mechanism and this follows next in the sequence of the phase diagram.

Somewhere in the vicinity of the periods of the most intense monsoon trough and of the Mascarene high, one should perhaps find the most intense cross-equatorial low-level jet. We do not present this in our diagram since we did not have observations for the same year. With the gradual buildup of the local Hadley-type overturning and widespread rainfall, it is not surprising that the Tibetan high attains its maximum intensity soon thereafter, and is followed by a buildup in the meridional pressure gradient and an increase in the intensity of the tropical easterly jet.

The maximum in the central Indian rainfall is an interesting problem, which is the last item in the phase diagram. Central India receives much of its intense rainfall from monsoon depressions. We feel that the problem of the formation and passage of *monsoon depressions deserves to be examined within the context of the phase cycle presented here.* During 1967 there were four major monsoon depressions that passed through central India. The dates of occurrence of these are plotted on the phase diagram by a star. The dates when they arrived near central India were 30 June, 27 July, 1 August and 20 August. One of these depressions developed just after the 27 July depression had moved over central India and produced some rainfall over central India on 1 and 2 August. There were also a number of monsoon lows (weaker than the depression) that passed through central India and contributed to the large rainfall totals shown in Fig. 15a. It is perhaps safe to state that the 13.1-day mode in the central Indian rainfall comes primarily from the contribution of these monsoon depressions and is only partly due to the passage of monsoon lows. We can, in principle, assign calendar dates on the phase diagram noting that our starting date, i.e, day 0, corresponds to 31 May 1967. Based on this we can see that three out of a possible maximum of four major depressions (see star location in Fig. 18a) formed after the major intensification of the elements of the monsoon system during its stabilizing phase. It would be presumptuous to state that monsoon depressions cause the cycle of events illustrated here. It is conceivable that instability mechanisms that are important for the formation of the monsoon depression are an integral part of this major oscillating monsoon system. The formation of a monsoon depression could then be viewed as a consequence of the periodic growth of the broad-scale instability mechanism.

## 5. Concluding remarks

In this paper we have examined the time series of thermodynamic instability parameters such as dry and moist static stability. It would be desirable to

carry out a similar analysis for dynamic stability parameters such as barotropic stability, combined barotropic-baroclinic instability, and possibly also a CISK (conditional instability of the second kind) parameter. It is our feeling that they probably also grow and decay in such a phase diagram. Such studies will provide a better understanding of phenomena such as the monsoon depression. Presently available data sets are not adequate to carry a careful analysis of such elements. However, we hope that this may be possible during the forthcoming GARP (Global Atmospheric Research Program) Monsoon Experiment (MONEX).

The salient results of spectral analysis are that the elements of the monsoon system (Fig. 1) show an interesting oscillation in the quasi-biweekly period range of $14\pm2$ days. All of the elements of the monsoon system exhibit distinct fluctuations around this time scale. There are also shorter time-scale fluctuations in the time frame of 2–6 days. The latter may be a reflection of local instabilities and local disturbance passages. The near two-week period oscillation of the monsoon system is of primary interest to us. In this study we have presented a sequential ordering of phase of these monsoon elements. It is worth emphasizing here that the aforementioned oscillation in the quasi-biweekly range seems to occur during years of near-normal rainfall. In order to study the oscillation of a monsoon system during a drought year much longer records are currently being examined. A number of possible reasons can be offered for this phenomenon. The following three possibilities are explored and discussed in part II of this paper.

1) Response of the monsoon system to winter hemisphere disturbances. A spectral analysis of global data in the Southern Hemisphere will be presented. Propagating waves, following Hayashi's (1971) procedure, exhibit quasi-biweekly modes. The passage of these disturbances could intensify the Mascarene high periodically, which in turn could intensify the low-level jet, the monsoon trough, monsoon convection, the Tibetan high, the tropical easterly jet, and so on. Such a sequence of events may not be consistent with the evolution of phase presented here.

2) Planetary-scale propagating waves in the pressure and satellite brightness over the Northern Hemisphere global tropics. We shall also present evidence of quasi-biweekly oscillations and zonal wave propagation of these elements.

3) A third approach toward the understanding of the quasi-biweekly oscillation is proposed here as a "natural oscillation" of the monsoon system. Here we shall present the results of long-term numerical integration of a zonally symmetric monsoon model which is an extension of the Murakami *et al.* (1970) paper. The oscillation occurs in the following manner. Net radiative effects warm the earth's surface, the heat balance of which includes both sensible and evaporative fluxes. The fluxes gradually build dry and moist instabilities in the lower layers. Heat is transported up by the dry and moist convective adjustment process. The heating is also augmented by large-scale condensation. As convection and condensation increase, cloudiness increases in the model. The gradual increase of cloudiness results in a gradual decrease in the incoming shortwave radiation reaching the earth's surface. As a consequence, there occurs a gradual stabilizing of the lower layer and the dry and moist convective processes slowly decrease and the associated cloud cover also starts to decrease. The shortwave radiation now starts to become effective once again and the cycle starts all over again.

*Acknowledgments.* The data for this study came from a number of different sources. We acknowledge the assistance of Mr. Findlater of the East African Meteorological Community, Mr. Beenay Pathack of the Mauritius Weather Service, the India Meteorological Department and Mr. Roy Jenne (NCAR). The research work reported here was supported by the Atmospheric Science Section of the National Science Foundation under Grant ATM75-18945. Computations were carried out on Florida State University's CDC 6400 and on the CDC 6600/7600 system of the National Center for Atmospheric Research which is sponsored by the National Science Foundation.

## REFERENCES

Chin, P. C., and M. H. Lai, 1974: Monthly mean upper winds and temperature over southeast Asia and the western North Pacific. *Roy. Observ. Tech. Memo.*, No. 12, Hong Kong, 1–115.

Colton, D. E., 1973: Barotropic scale interactions in the tropical upper troposphere during the northern summer. *J. Atmos. Sci.*, **30**, 1287–1302.

Endlich, R. M., R. C. Singleton and J. W. Kaufman, 1969: Analysis of detailed vertical wind speed profiles. *J. Atmos. Sci.*, **26**, 1030–1041.

Findlater, J., 1969a: A major low-level air current near the western Indian Ocean during the northern summer. *Quart. J. Roy. Meteor. Soc.*, **95**, 362–380.

——, 1969b: Interhemispheric transport of air in the lower troposphere over the western Indian Ocean. *Quart. J. Roy. Meteor. Soc.*, **95**, 400–403.

——, 1971: Mean monthly air flow at low levels over the western Indian Ocean. *Geophys. Mem.*, No. 115, HMSO, London.

Flohn, H., 1968: Contribution to a meteorology of the Tibetan Highlands. Rep. No. 130, Dept. Atmos. Sci., Colorado State University, Fort Collins, 1–120.

Gruber, A., 1974: The wavenumber-frequency spectra of satellite measured brightness in the tropics. *J. Atmos. Sci.*, **31**, 1675–1680.

Hayashi, Y., 1971: A generalized method of resolving disturbances into progressive and retrogressive wave by space Fourier and time spectral analyses. *J. Meteor. Soc. Japan*, **49**, 125–128.

Kanamitsu, M., T. N. Krishnamurti and C. Depradine, 1972: On scale interaction in the tropics during northern summer. *J. Atmos. Sci.*, **29**, 698–706.

Koteswaram, P., 1961: The easterly jet stream in the tropics. *Tellus*, **10**, 43–57.

Krishnamurti, T. N., 1971: Observational study of tropical upper tropospheric motion field during Northern Hemisphere summer. *J. Appl. Meteor.*, **10**, 1066–1096.

——, and E. D. Rodgers, 1970: 200 mb wind field June, July, August 1967. Tech. Rep. No. 70-2, Meteor. Dept., Florida State University, 161 pp.

——, and M. Kanamitsu, 1973: A study of a coasting easterly wave. *Tellus*, **25**, 568–586.

——, J. Molinari and H. Pan, 1976: Numerical simulation of the Somali jet. (Submitted for publication to *J. Atmos. Sci.*)

——, S. M. Daggupaty, J. Fein, M. Kanamitsu and J. D. Lee, 1973: Tibetan high and upper tropospheric tropical circulation during northern summer. *Bull. Amer. Meteor. Soc.*, **54**, 1234–1239.

Murakami, M., 1976: Analysis of summer monsoon fluctuations over India. *J. Meteor. Soc. Japan*, **54**, 15–31.

Murakami, T., and M. Frydrych, 1974: On the preference period of upper wind fluctuations during the summer monsoon. *J. Atmos. Sci.*, **31**, 1549–1555.

——, R. Godbole and R. R. Kelkar, 1970: Numerical simulation of the monsoons along 80°E. *Proc. Conf. on Summer Monsoon of Southeast Asia*, Navy Weather Research Facility, Norfolk, Va., 39–51 [Available from the Naval Environmental Prediction Group, Navy Postgraduate School, Monterey, Calif.].

Ramamurthy, K., 1969: Some aspects of the break in the Indian southwest monsoon during July and August. Forecasting Manual No. IV-18.3, India Meteor. Dept., Poona, 1–57.

Wallace, J. M., 1971: Spectral studies of tropospheric wave disturbances in the tropical western Pacific. *Rev. Geophys. Space Phys.*, **9**, 557–612.

Warsh, K. L., K. L. Echternacht and M. Garstang, 1971: Structure of near surface currents east of Barbados. *J. Phys. Oceanogr.*, **1**, 123–129.

Yanai, M., T. Maruyama, T. Nitta and Y. Hayashi, 1968: Power spectra of large-scale disturbances over the tropical Pacific. *J. Meteor. Soc. Japan*, **46**, 308–323.

Zangvil, A., 1975: Upper tropospheric waves in the tropics and their association with clouds in the wavenumber-frequency domain. Ph.D. thesis, University of California, Los Angeles, 131 pp.